Int. J. Solids Structures Vol. 17, pp. 687–697, 1981
Printed in Great Britain.

0020-7683/81/070687-11$02.00/0
Pergamon Press Ltd.

DOUBLY ASYMPTOTIC, BOUNDARY-ELEMENT ANALYSIS OF DYNAMIC SOIL-STRUCTURE INTERACTION†

PHILIP UNDERWOOD and T. L. GEERS
Lockheed Palo Alto Research Laboratory, 3251 Hanover Street, Palo Alto, CA 94304, U.S.A.

(*Received* 29 *January* 1980; *in revised form* 18 *August* 1980)

Abstract—This paper describes a doubly asymptotic (DA), boundary-element (BE) treatment of dynamic soil-structure interaction where the surrounding medium is treated as linear-elastic. The interaction is reduced to a surface relationship that is asymptotically exact at both high and low frequencies. Governing equations are developed in matrix form for application to complex structures. Numerical results are presented for a two-dimensional problem for which analytical solutions have appeared in the literature. Good agreement between the DA/BE and analytical results is observed.

INTRODUCTION

The treatment of soil-structure interaction is of considerable importance in analyses of the integrity of structures in ground-shock environments. There are currently three basic approaches to the linear treatment of this problem: analytical, lumped-element and finite-element. Analytical approaches are restricted to very simple geometries; hence, the results are useful for providing insight into the physics of the problem, but the extension to complex geometries is difficult. The lumped-element approach, in which the soil characteristics are represented by discrete masses, springs and dashpots, is economical, but the representation of actual soil behavior is crude. The finite-element (FE) approach can model the problem to almost any accuracy desired, but the large number of elements required precludes efficient computation. An approach to achieve a more versatile and more economical method for the treatment of these problems would combine the best features of the different techniques. Such an approach is pursued in this study: an analytical approximation of the soil-structure interaction is combined with the modeling capabilities of the FE method, while avoiding the burden of many elements in the soil.

This paper examines a linear boundary-element (BE) treatment of the surrounding soil that offers considerable promise for complex soil-structure dynamic analysis. The structure is modeled through the use of an available FE code and the soil-structure interaction is reduced to a surface relationship through the use of a doubly asymptotic approximation (DAA)[1], which requires the application of BE techniques[2]. The present study focuses on the two-dimensional plane-strain response of structures surrounded by an infinite elastic medium; the extension to more general problems is discussed. The paper first addresses the development of the method: the matrix equation of motion for a structure embedded in an elastic medium is given, the doubly asymptotic surface relationship is presented and the response equation for the embedded structure is synthesized. Then the solution procedure is discussed, and three numerical examples are considered that illustrate the validity and accuracy of the approach.

A DA/BE approach to problems of this class possesses some distinctively attractive features. First, the governing equations of the discrete soil-structure system are frequency-independent and are therefore suitable for transient response analysis by direct time integration. This is in contrast to frequency-dependent methods[3, 4] which require that the analysis be performed in the frequency domain, thereby inhibiting extension to nonlinear analysis. Second, the physical properties of the soil-structure interaction are represented by uniquely defined damping and stiffness coefficients; hence "tuning" of a model is not necessary to achieve proper radiation and stiffness behavior, as it is with infinite elements[5] and other frequency-independent methods, e.g.[6]. Third, the resulting equations of motion are the

†Portions on this paper were presented at the Sixth Canadian Congress of Applied Mechanics, 30 May–3 June 1977, University of British Columbia, Vancouver, Canada.

classical second-order equations of structural dynamics, so no special time integration scheme is required for numerical solution, as may be required by nonreflecting boundary formulations[7]. A good review of current methods for the computational treatment of wave propagation in infinite domains is given by Zienkiewicz *et al.*[8].

GOVERNING EQUATIONS

In this section, governing equations for a finite-element (FE) model of a structure and a boundary-element (BE) formulation of a first-order doubly asymptotic approximation (DAA) for the soil-structure interaction are provided. These equations are then combined to form the response equation for the embedded structure. Finally, computational procedures for the solution of the response equation are discussed.

Structural model

The matrix FE equation of motion for a linear structure embedded in an elastic medium through which an incident disturbance propagates is

$$\underline{M}_s\ddot{\underline{q}} + \underline{K}_s\underline{q} = -(\underline{f}_I + \underline{f}_S) \tag{1}$$

where $\underline{M}_s$ and $\underline{K}_s$ are the mass and stiffness matrices for the structure, $\underline{q}$ is the structural displacement vector, $\underline{f}_I$ and $\underline{f}_S$ are surface-force vectors associated with the incident and scattered waves, respectively and a dot denotes temporal differentiation. The mass and stiffness matrices are easily obtained from any available FE code. The applied load is considered separable into an incident-wave force that would exist if the structure were absent (hence a known quantity) and a scattered-wave force due to the presence of the structure. The scattered-wave force constitutes a troublesome unknown; hence an approximation is introduced for its evaluation.

Doubly asymptotic approximation

A first-order DAA is introduced to evaluate the scattered-wave force $\underline{f}_S$[1]. This approximation is a surface interaction approximation, replacing the infinite volume of external medium by a surface coincident with the external surface of the structure. The approximation is asymptotically valid at both high and low frequencies, as are the previously developed approximations for fluid-structure interaction[9–11].

The development of a first-order DAA for linear soil-structure interaction proceeds as follows. At high frequencies, each surface element of the discretized structure acts as an infinite flat plate radiating plane waves into the medium. This can be visualized by considering that, for a fixed surface-vibration pattern oscillating at high frequencies, the characteristic propagation wave lengths in the medium are short compared with the characteristic wavelength of the surface-vibration pattern. For nornal and tangential motions of the ith surface element, this model yields as scattered-wave surface forces

$$\begin{aligned} g^n_{Si} &= \rho c_d a_i \dot{u}_i^n \\ g^t_{Si} &= \rho c_s a_i \dot{u}_i^t \end{aligned} \tag{2}$$

where ρ is the mass density of the medium, a_i is the surface area of the element, c_d and c_s are the propagation sounds for dilatational and shear waves in the medium, respectively and $\dot{u}_i^n$ and $\dot{u}_i^t$ are the normal and tangential scattered velocities at the surface of the element; see, e.g.,[6]. For an assemblage of elements, (2) lead to the matrix relation

$$\underline{g}'_S = \rho \underline{A}\underline{C}_m \dot{\underline{u}}'_S \tag{3}$$

where $\underline{A}$ is a diagonal element-area matrix, $\underline{C}_m$ is a diagonal sound-speed matrix for the medium and $\dot{\underline{u}}'_S$ is the computational scattered-velocity vector for the surface elements

expressed in *local* coordinates. Upon assembly, the local coordinates in (3) are transformed to the *global* coordinates for the problem as

$$\underline{u}_S = \underline{G}\underline{u}_S. \tag{4}$$

From (3), it is clear that the external medium appears to the structure as an array of dashpots in the high-frequency limit.

Low-frequency behavior of the medium is described by the quasi-static surface relation

$$\underline{g}_S = \underline{K}_m\underline{u}_S \tag{5}$$

in which $\underline{K}_m$ is a surface stiffness matrix for the medium. The construction of $\underline{K}_m$ is discussed below. In this limit, it is clear that the external medium appears to the structure as an array of springs.

To construct the first-order DAA, (3) and (5) are combined to obtain

$$\underline{g}_S = \rho\underline{G}^T\underline{A}\underline{C}_m\underline{G}\dot{\underline{u}}_S + \underline{K}_m\underline{u}_S \tag{6}$$

where the transformation of (3) as $g_S = G^T g'_S$ results from (4) and the fact that virtual work must be independent of the coordinate system used, i.e. $(\delta\underline{u})^T\underline{g} = (\delta\underline{u}')^T\underline{g}'$. It is easy to see the doubly asymptotic nature of the surface approximation. At low frequencies, the velocity vector is small relative to the displacement vector, so that the scattered force is essentially given by the static stiffness relationship; at high frequencies, the reverse is true, so that the scattered force is essentially given by the radiation damping relationship. In the intermediate frequency range, the DAA is, of course, in error; the purpose of the numerical results presented herein is to indicate the magnitude of that error. If numerical calculations demonstrate the need for an improved approximation, one may be derived; for fluid-structure interaction, an improved DAA has been developed that substantially outperforms the original[11].

Response equation

For linear problems, not only is the surface-force vector separable into incident-wave and scattered-wave components [see (1)], but the surface displacement vector $\underline{u}$ is also separable such that $\underline{u} = \underline{u}_I + \underline{u}_S$[12]. Hence (1) and (6) may be combined to give the doubly asymptotic response equation for the embedded structure

$$\underline{M}_s\ddot{\underline{q}} + \rho\underline{D}^T\underline{G}^T\underline{A}\underline{C}_m\underline{G}\underline{D}\dot{\underline{q}} + (\underline{K}_s + \underline{D}^T\underline{K}_m\underline{D})\underline{q} = -\underline{f}_I + \rho\underline{D}^T\underline{G}^T\underline{A}\underline{C}_m\dot{\underline{u}}_I + \underline{D}^T\underline{K}_m\underline{u}_I \tag{7}$$

where $\underline{u}$ and $\underline{f}_S$ have been transformed as $\underline{u} = \underline{D}\underline{q}$ and $\underline{f}_S = \underline{D}^T\underline{g}_S$. In (7) $\underline{D}$ is the soil-structure transformation matrix that relates the boundary-element and finite-element degrees of freedom, $\underline{M}_s$ and $\underline{K}_s$ are readily provided by an FE structural analysis code, $\underline{D}^T\underline{G}^T\underline{A}\underline{C}_m\underline{G}\underline{D}$ is easily computed, $\underline{f}_I$ and $\underline{u}_I$ are known and K_m is determined through the application of boundary-integral-equation techniques, as now described.

For nonlinear problems, perhaps the most straightforward extension of (7) for the treatment of nonlinear soil behavior consists merely of including an "island" of non-linear medium surrounding the embedded structure as part of that structure. Hence the soil in the immediate vicinity of the structure is modeled by nonlinear FE techniques, while the remaining soil of infinite extent is modeled by the linear DA/BE technique.

Medium stiffness matrix

The basic two-dimensional boundary-integral equation for the surface behavior of an elastic medium is[13]

$$\frac{1}{2}u^k(P) + \int_L T^{kl}(P, Q)u^l(Q)\,dL(Q) = \int_L U^{kl}(P, Q)t^l(Q)\,dL(Q) \tag{8}$$

where P and Q are surface points, u^k and t^k are surface displacements and tractions,

respectively, T^{kl} and U^{kl} are Green's functions for the boundary and $k = 1, 2$ and $l = 1, 2$ are the Cartesian coordinate indices. Through representation of the structure's (two-dimensional) external surface by an array of boundary elements, (8) may be expressed in matrix notation as

$$\underline{S}\underline{u} = \underline{F}\underline{t} \tag{9}$$

in which the 2×2 elements of $\underline{S}$ and $\underline{F}$ are given by

$$S_{ij}^{kl} = \frac{1}{2}\delta_{ij}\delta_{kl} + \int_{L_j} T_{ij}^{kl}\zeta_j^l \, dL_j$$

$$F_{ij}^{kl} = \int_{L_j} U_{ij}^{kl}\zeta_j^l \, dL_j \tag{10}$$

where δ_{ij} and δ_{kl} are Kronecker deltas, i and j are boundary-element indices, ξ_j^l and ζ_j^l are assumed BE shape-functions and L_j is the length of the jth boundary element. For the two-dimensional plane-strain case, the kernels T_{ij}^{kl} and U_{ij}^{kl} are given by[2, 13]

$$T_{ij}^{kl} = \frac{C_3}{r_{ij}}\left[\frac{\partial r_{ij}}{\partial n_j}(\delta_{kl}C_4 + 2r_{ij,k}r_{ij,l}) + C_4(n_j^k r_{ij,l} - n_j^l r_{ij,k})\right]$$

$$U_{ij}^{kl} = C_1(\delta_{kl}C_2 \ln r_{ij} - r_{ij,k}r_{ij,l}) \tag{11}$$

where C_1, C_2, C_3 and C_4 are material constants, r_{ij} is the distance from a node point on the ith element to the field point of integration on the jth element, n_j is the unit normal to the surface of the jth element, n_j^k is the cosine of the angle between n_j and the kth Cartesian direction and a subscript following a comma represents spatial differentiation with respect to the indicated Cartesian coordinate at point j. In the present implementation, the displacement and traction shape-functions ξ_j^k and ζ_j^k are assumed to be constant over the jth element, so they may be brought out from under the integral signs in (10). The numerical techniques used to evaluate the integrals in (10) are discussed in the appendix.

Once the matrices in (9) have been generated, it is a simple matter to obtain the medium stiffness matrix; because F is nonsingular, it can be factored to obtain

$$\underline{t} = \underline{F}^{-1}\underline{S}\underline{u} = \underline{K}_m\underline{u}. \tag{12}$$

As the preceding development is not based on variational principles, the derived stiffness matrix may not be symmetric. For explicit time integration, this is immaterial; for implicit integration, a nonsymmetric equation solver may be used, or $\underline{K}_m$ may be symmetrized by various methods[14].

The brevity of the preceding BE formulation is appropriate, in view of the extensive coverage of the subject provided in [2]. The emphasis here has been on the specific approach of this study; it has been found to be most economical, especially the use of numerical integration to evaluate the matrix elements defined in (10). The apparently new technique of using boundary integral equations to define a medium stiffness matrix is valuable, in that it facilitates the use of the form (12). This form is required for an efficient marriage of an FE structural model and a BE soil model. There are also improved forms of the BE method available that utilize higher order shape functions to describe boundary displacements and tractions, as well as sophisticated isoparametric-element representations; these procedures are reviewed by Cruse[15]. The simple approach used in this study is quite satisfactory for the purposes of the present investigation. If software were to be constructed for production analysis, the incorporation of refined BE techniques would be appropriate.

Solution procedure

The doubly asymptotic response equation for the embedded structure, (7), has the form of the standard matrix equation of structural dynamics; hence the solution of (7) may be accomplished with well-established techniques. For the linear response problems considered

here, the integration of (7) is performed in accordance with the trapezoidal rule[16]. The equation solver used with the time integrator is the skyline format procedure[17].

An examination of (7) on a term-by-term basis is informative. The mass matrix produced by REXBAT[18], the structural finite-element code used in this study, is diagonal; a consistent mass matrix could be used, however, without unduly complicating the solution. The damping matrix is highly banded in all cases and presents no computational difficulties. The stiffness matrix, on the other hand, may be nearly full, due to the added stiffness terms [see (10)]. For simple examples considered here, the nonbanded combined-stiffness matrix presents no difficulty. For large systems, however, the compact-bandwidth (low-connectivity) advantage of the structural model, which is needed for efficient solution, would be lost through the addition of the fully populated added stiffness matrix. To overcome this problem, a staggered-solution approach, such as the one developed for fluid-structure interaction analysis in [19], should be considered for large systems of equations. The forcing function, i.e. the right side of (7), may look complicated, but each term is known and the load vector is easily computed by simple matrix-vector multiplication and vector addition.

NUMERICAL RESULTS

In this section, numerical results for the plane-strain response of an infinite, circular cylindrical cavity and an infinite, circular cylindrical shell are compared with corresponding analytical solutions. Problem geometry and notation are shown in Fig. 1; in all cases, excitation is provided by a plane dilational wave. The coincident finite-element and boundary-element grids for the three problems considered consist of 40 elements of equal length. The finite-element shell models incorporate straight beam elements with elastic moduli modified for representation of plane-strain conditions. Note that for this geometry $\underline{K}_m$ is symmetric.

The results are presented in nondimensional form. Length is normalized to a, time is normalized to a/c_d, and stress is normalized to $\rho c_d^2 = \lambda + 2\mu$, where λ and μ are the Lamé coefficients for the medium.

Incident wave

A plane dilatational step-wave, characterized by a compressive pressure P_0 and moving in

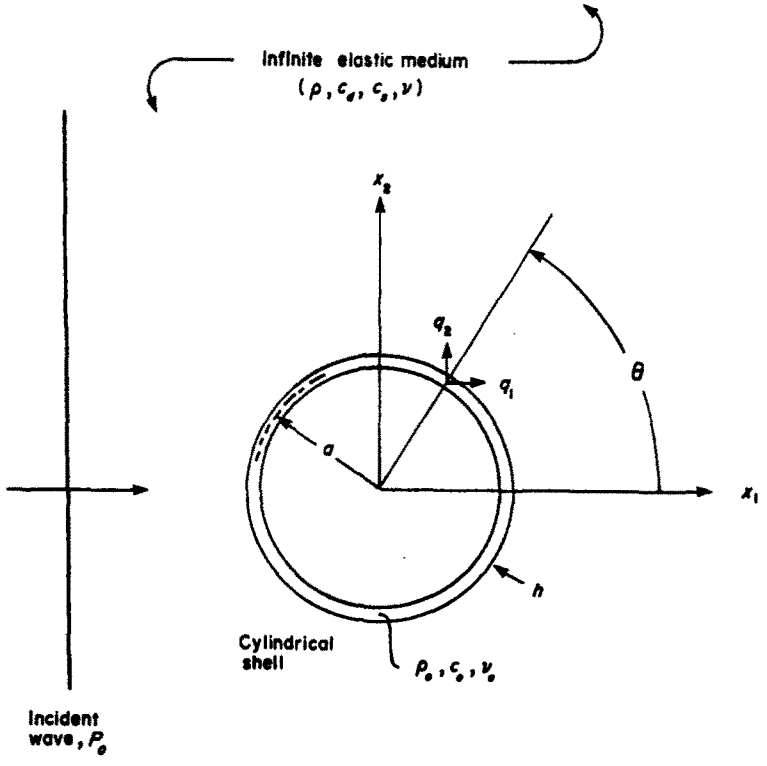

Fig. 1. Geometry and notation for the check problems.

the x_1-direction, can be described in terms of a nondimensional scalar potential ϕ_I as

$$\phi_I = -\frac{1}{2} P_0(\tau - x_1 - 1)^2 H(\tau - x_1 - 1) \tag{13}$$

where τ is nondimensional time, x_1 is nondimensional position along the x_1 axis and H is the Heaviside operator. For this incident wave, the shear potential is zero[12].

The incident-wave force vector f_I, which appears on the right side of (7), is obtained as follows. First, the elements of the incident-wave computational stress vector in global (x_1, x_2) coordinates are determined by application of classical continuum formulas to (13)[12]; this yields

$$\begin{aligned} \sigma_{Ii}^k &= -(\lambda + 2\mu\delta_{1k}) P_0 H(\tau - x_{1i} - 1) \\ \tau_{Ii}^{kl} &= 0 \end{aligned} \tag{14}$$

where x_{1i} denotes the x_1-position of the ith surface mode. Second, a global stress vector is constructed from these elements, which is then transformed, on the basis on Mohr's circle, into local coordinates as $\underline{\sigma}'_I = \underline{M}\underline{\sigma}_I$. Finally, the force vector in local coordinates is determined as $\underline{f}'_I = -\underline{A}\underline{\sigma}'_I$, which is then transformed into global coordinates; all the yields

$$\underline{f}_I = -\underline{G}^T \underline{A} \underline{M} \underline{\sigma}_I. \tag{15}$$

The incident-wave displacement and velocity vectors $\underline{u}_I$ and $\dot{\underline{u}}_I$, which also appear on the right side of (7), are obtained from the classical relation $u^k = \partial\phi/\partial x_k$. This relation and (13) yield as the elements of these vectors

$$\begin{aligned} u_{Ii}^k &= \delta_{1k} P_0(\tau - x_{1i} - 1) H(\tau - x_{1i} - 1) \\ \dot{u}_{Ii}^k &= \delta_{1k} P_0 H(\tau - x_{1i} - 1). \end{aligned} \tag{16}$$

Circular cavity

The cavity problem is formulated simply by taking $\underline{M}_s = \underline{K}_s = 0$, which reduces (7) to a first-order equation. A comparison between results obtained by the present method and analytical results presented in [20] is provided, for step-wave excitation, in Fig. 2. Minor discrepancies exist between the DA/BE and analytical response histories at early times. At late times, both sets of response histories approach the appropriate asymptotes[1, 21]; these asymptotes are $\tau - 4$, $\tau - 1$ and $\tau + 2$ for $\theta = 0°$, 90° and 180°, respectively.

Concrete shell in slow granite

The second check problem, the response of a concrete shell to an incident wave of rectangular stress profile, is also taken from [20]. The nondimensional parameters for this problem are $h/a = 0.01$, $\rho_0/\rho = 0.865$, $c_s/c_d = 0.63$, $c_0/c_d = 1.87$, $\nu = 0.25$ and $\nu_0 = 0.2$; the duration of the incident rectangular pulse is 10. DA/BE and analytical displacement histories for this problem are compared in Fig. 3. In this figure, as in Fig. 2, the DA/BE responses generally tend to lag behind their analytical counterparts. As discussed in [1], this tendency is the result of excess radiation damping introduced by the DAA. Also of interest is the DA/BE prediction of shell response at $\theta = 0°$ before $\tau = 1.53$, which is the earliest time a disturbance can reach that point[22]; this nonphysical result illustrates that, strictly speaking, the DAA is not a wave propagation approximation. Despite its deficiencies, however, the DAA produces results that nowhere differ from their analytical counterparts by more than 10% of the peak response and also approach the proper late-time asymptote. The latter characteristic attests to the correctness of the $\underline{K}_m$-calculation.

Although the DAA tends to overestimate radiation damping, its inclusion is absolutely necessary for an accurate treatment of abrupt soil-structure interaction. This is indicated in Fig.

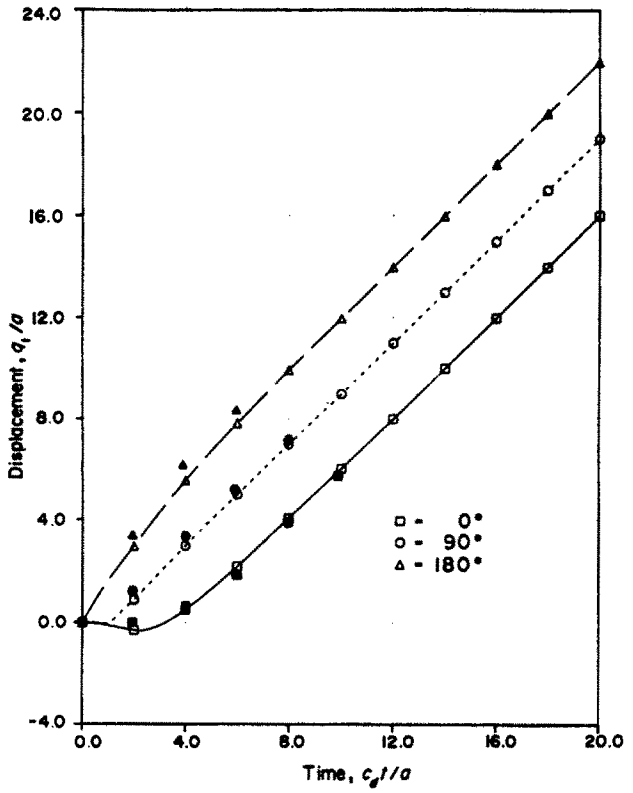

Fig. 2. Displacement response of a circular cavity of an incident step-wave. (Solid symbols denote results from [20]).

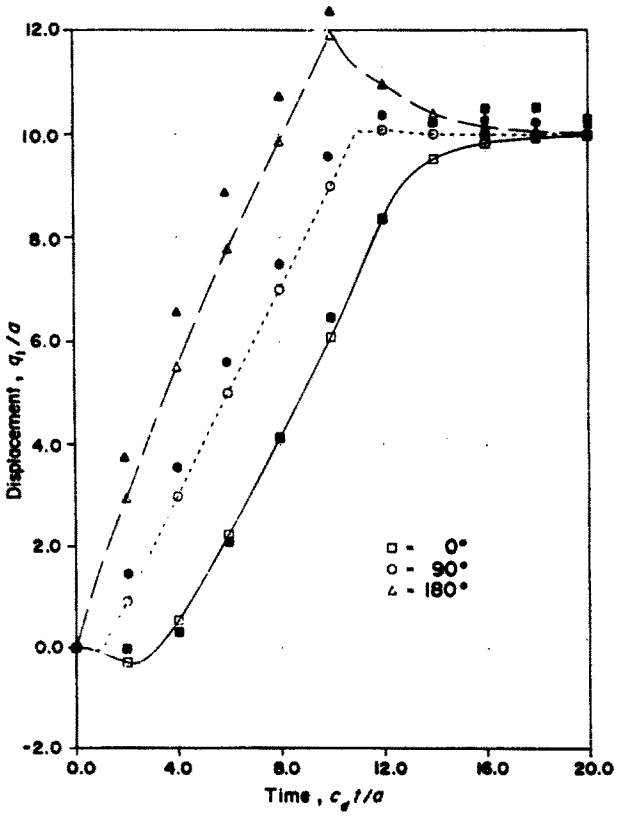

Fig. 3. Displacement response of a concrete shell in slow granite to an incident wave of rectangular stress profile. (Solid symbols denote results from [20]).

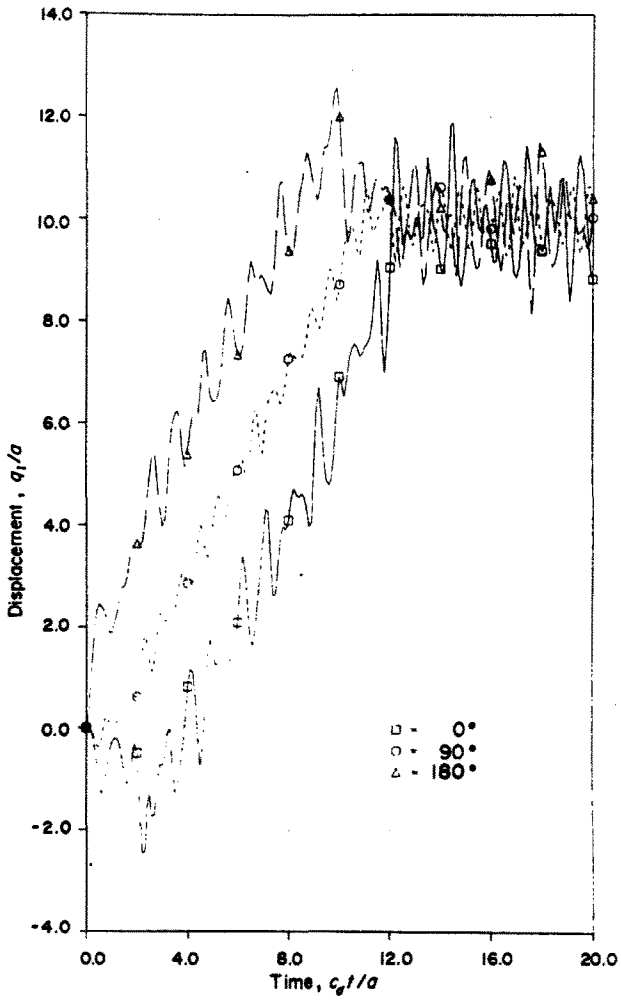

Fig. 4. Displacement response of the concrete shell in slow granite computed with $C_m = 0$.

4, where displacement responses corresponding to the DA/BE responses of Fig. 3 have been computed from (7) with C_m set equal to 0. As one would expect, the highly oscillatory response thus calculated produces extremely poor stress/strain results.

Concrete shell in granite

The final check problem, the response of a concrete shell to an incident step-wave, is taken from [1]. The appropriate nondimensional parameters here are $h/a = 0.5$, $\rho_0/\rho = 1.0$, $c_s/c_d = 1/\sqrt{3}$, $c_0/c_d = 1/\sqrt{2}$ and $\nu = \nu_0 = 0.25$. Velocity response histories at $\theta = 0°$ and 180° are shown in Fig. 5, corresponding to DA/BE, DA/analytical and exact/analytical treatments of the structure-medium interaction. Although it is difficult to see in Fig. 5, the peak velocity for DA/BE (180°) is 2.02 and for DA/analytical (180°) is 2.09; thus it is seen that the DA/BE and DA/analytical results are in almost perfect agreement, which is most reassuring. Premature initial response at points in the shadow region and excessive radiation camping characterize the DA results here as they did in Fig. 3. The associated error is modest, however, with all results coalescing at late times. Stress response histories in the middle and inner fibers of the shell at $\theta = 90°$ are shown in Fig. 6. Here, some minor discrepancies between the DA/BE and DA/analytical results appear: near $\tau = 0$, the DA/BE histories exhibit a more realistic delay before a stress response appears; near $\tau = 1.5$, short-term reversals in stress appear in the DA/BE histories, whereas the analytical histories are smooth; finally, at late times, the DA/BE asymptotic stress values are slightly less than their analytical counterparts. Much larger discrepancies exist between the DA results and the exact results, especially during the period $4 \lesssim \tau \lesssim 12$. Even here, however, the error never exceeds 15%, which is generally acceptable for engineering analysis.

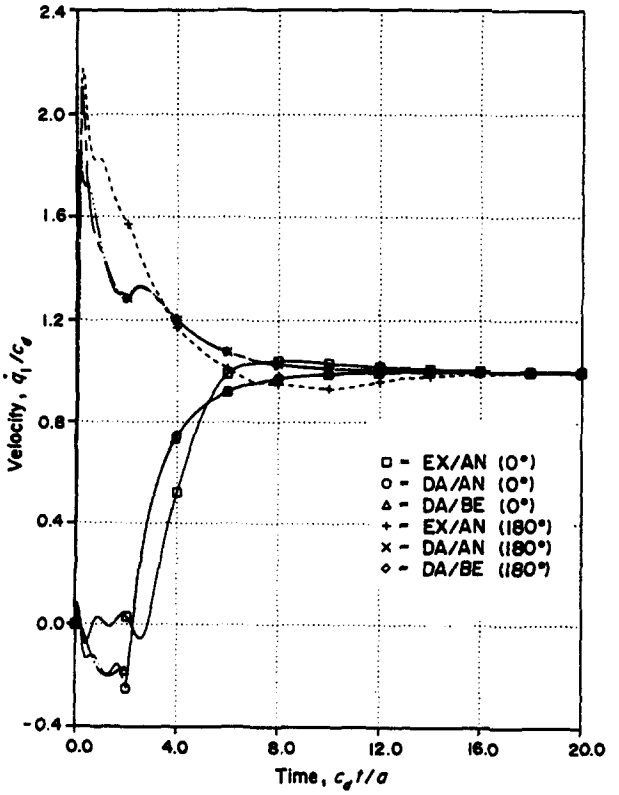

Fig. 5. Velocity response of a concrete shell in granite to an incident step-wave.

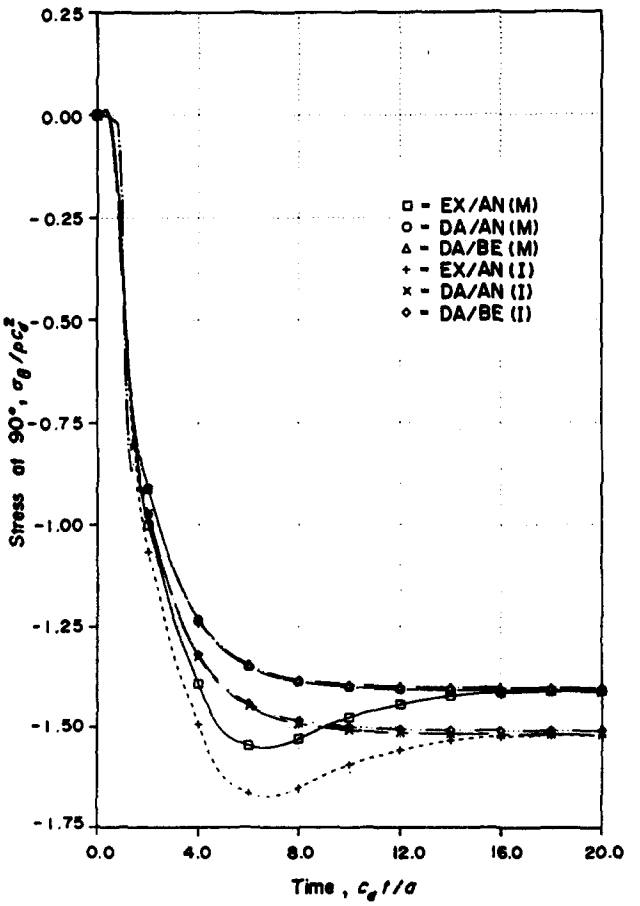

Fig. 6. Stress response in the middle and inner fibers of a concrete shell in granite to an incident step-wave.

CONCLUSION

The preceding numerical results indicate that the doubly asymptotic approximation of [1] offers considerable promise for the satisfactory treatment of dynamic soil-structure interaction, and that the DA/BE method described above is suitable for application to engineering structures with complex surface geometries. Extension of the DA/BE method for the treatment of nonlinear soil behavior is most easily accomplished via the concept of a soil island with a DA/BE surface. The extension to problems involving elastic half-spaces is currently being studied.

Acknowledgements—The authors express their appreciation to Drs. J. A. DeRuntz, C. A. Felippa and K. C. Park and to Mr. E. M. Olsen, for valuable consulatation on the intricacies of boundary integral equations and their numerical solution. A debt is also owed to Dr. C.-L. Yen for providing analytical check results. This study was funded by the Defense Nuclear Agency under Contract number DNA001-75-C-0294.

REFERENCES

1. T. L. Geers and C.-L. Yen, Transient excitation of cylindrical and spherical shells embedded in elastic media: Residual potential and doubly asymptotic solutions, LMSC-D767735. Lockheed Palo Alto Research Laboratory, Palo Alto, CA. (Feb. 1981).
2. T. A. Cruse and F. J. Rizzo (Eds), *Boundary Integral Equation Method: Computational Applications in Applied Mechanics*, AMD-Vol. 11. ASME, New York (1975).
3. F. E. Richart, Jr., J. R. Hall, Jr. and R. D. Woods, *Vibrations of Soils and Foundations*. Prentice-Hall, Englewood Cliffs, New Jersey (1970).
4. A. S. Veletsos and V. V. D. Nair, Torsional vibration of viscoelastic foundations. *J. Geotech. Engng Div. ASCE* **100**(GT3), 225–246 (March 1974).
5. P. Bettess, Infinite elements. *Int. J. Num. Meth. Engng* **11**(1), 53–64 (1977).
6. J. Lysmer and R. L. Kuhlemeyer, Finite dynamics model for infinite media. *J. Engng Mech. Div. ASCE* **94**(EM4), 869–877 (Aug. 1969).
7. P. A. Cundall, R. R. Kunar, P. C. Carpenter and J. Marti, Solution of infinite dynamic problems by finite modeling in the time domain. Proceedings of 2nd International Conference on Applied Numerical Modellings Madrid, Spain, (September 1978).
8. O. C. Zienkiewicz, D. W. Kelley and P. Bettess, The Summerfeld (radiation) condition on infinite domains and its modeling in numerical procedures. *Lecture Notes in Mathematics*, 704 (Edited by R. Glowinski and J. L. Lyons), pp. 169–203. Springer-Verlag, Berlin (1979).
9. T. L. Geers, Residual potential and approximate methods for three-dimensional fluid-structure interaction problems. *J. Acoust. Soc. Am.* **49**, 1505–1510 (1971).
10. T. L. Geers, Transient response analysis of submerged structures. *Finite Element Analysis of Transient Nonlinear Structural Behavior*, AMD-Vol. 14, pp. 59–84. ASME, New York (1975).
11. T. L. Geers, Doubly asymptotic approximations for transient motions of submerged structures. *J. Acoust. Soc. Am.* **64**, 1500–1508 (1978).
12. J. D. Achenbach, *Wave Propagation in Elastic Solids*. North-Holland, Amsterdam (1973).
13. F. J. Rizzo, An integral equation approach to boundary value problems of classical elastostatics. *Quart. Appl. Math.* **25**, 83–95 (1967).
14. O. C. Zienkiewicz, D. W. Kelley and P. Bettess, The coupling of the finite element method and boundary solution procedures. *Int. J. Num. Meth. Engng* **11**(2), 355–375 (1977).
15. T. A. Cruse and R. B. Wilson, Advanced applications of boundary integral equation methods. *Proc. 4th Int. Conf. on Structural Mech. in Reactor Technology*, San Francisco, pp. 15–19 (Aug. 1977).
16. C. A. Felippa and K. C. Park, Computational aspects of time integration procedures in structural dynamics. *J. Appl. Mech.* **45**, 595–611 (1978).
17. C. A. Felippa, Solution of linear equations with skyline-stored symmetric matrix. *Computers and Structures* **5**, 13–29 (1975).
18. W. A. Loden and L. E. Stearns, *User's Manual for the REXBAT Program*, LMSC-D460625. Lockheed Missiles & Space Co., Sunnyvale, CA (Jan. 1976).
19. K. C. Park, C. A. Felippa and J. A. DeRuntz, Stabilization of staggered solution procedures for fluid-structure interaction analysis. *Computational Methods for Fluid Structure Interaction Problems*, AMD-Vol. 26, pp. 95–124. ASME, New York (1977).
20. H. Garnet and J. Crouzet-Pascal, Transient response of a circular cylinder of arbitrary thickness, in an elastic medium, to a plane dilatational wave. *J. Appl. Mech.* **33**, 521–531 (1966).
21. T. Yoshihara, A. R. Robinson and J. L. Merritt, Interaction of plane elastic waves with an elastic cylindrical shell. *Structure Research Series Report No.* 261. University of Illinois, Urbana (Jan. 1963).
22. T. L. Geers, Scattering of a transient acoustic wave by an elastic cylindrical shell. *J. Acoust. Soc. Am.* **51**, 1640–1651 (1972).
23. G. Dahlquist and A. Bjork, *Numerical Methods*. Prentice-Hall, Englewood Cliffs, New Jersey (1974).

APPENDIX

This appendix discusses the numerical approach used to evaluate the integrals in (10) for determination of the matrix elements S_{ij}^{kl} and F_{ij}^{kl}.

First, the boundary is divided into 2-D boundary elements, each with a centrally located node. For a single calculation of S_{ij}^{kl} and F_{ij}^{kl}, fixed values are assigned to i, j, k and l, and a circle is fitted to the nodal points $j-1$, j and $j+1$; this completely determines the center and radius of the arc describing the jth element. The ends of the jth element are then point $j-\frac{1}{2}$ on the arc half-way between points $j-1$ and j and point $j+\frac{1}{2}$ on the arc half-way between points j and $j+1$.

Hence L_j is the arc length between points $j-\frac{1}{2}$ and $j+\frac{1}{2}$, and the unit normal anywhere on the element is completely defined.

Second, the displacement and traction shape functions, ξ_j^l and ζ_j^l, are taken as unity, so the integrals in (10) involve only the kernels (11). In this connection, it is important to remember that T_{ij}^{kl} and U_{ij}^{kl} pertain to a *fixed* point (the nodal point) on the ith element, but to a *variable* point on the jth element. For $j \neq i$, the geometric quantities in (11) are easily determined as

$$r_{ij} = [(x_{1i} - x_{1j})^2 + (x_{2i} - x_{2j})^2]^{1/2}$$
$$r_{ij,k} = (x_{kj} - x_{ki})/r_{ij}$$
$$\frac{\partial r_{ij}}{\partial n_j} = n_j^1 r_{ij,1} + n_j^2 r_{ij,2}. \tag{17}$$

Simpson's rule is used to evaluate the integrals with points $j-\frac{1}{2}$, j and $j+\frac{1}{2}$ as the integration points. For $j = i$, special evaluation methods are used, as described in the following paragraph.

With regard to the integral of T_{ii}^{kl}, it may be shown[13] that [see (11)]

$$\int_{L_i} r_{ii}^{-1} \frac{\partial r_{ii}}{\partial n_i} (\delta_{kl} C_4 + 2 r_{ii,k} r_{ii,l}) \, dL_i = -\pi (C_4 + 1) \delta_{kl}$$
$$\int_{L_i} (n_i^k r_{ii,l} - n_i^l r_{ii,k}) \, dL_i = 0 \tag{18}$$

where the first i-subscript of the doubly subscripted variable r_{ii} refers to the fixed nodal point for the ith element and the second i-subscript of r_{ii} and any single i-subscript refers to a variable point on that element. With regard to the integral of U_{ii}^{kl}, it may be shown that [see (11)]

$$\int_{L_i} \ln r_{ii} \, dL_i = r_{i(i-\frac{1}{2})}(\ln r_{i(i-\frac{1}{2})} - 1) + r_{i(i+\frac{1}{2})}(\ln r_{i(i+\frac{1}{2})} - 1) \tag{19}$$

where the subscripts $(i-\frac{1}{2})$ and $(i+\frac{1}{2})$ refer to the end points of the ith element. Integration of the second term in the expression for U_{ii}^{kl} [see (11)] is performed by means of Simpson's rule, with the nodal point i and the end points $i-\frac{1}{2}$ and $i+\frac{1}{2}$ as integration points. In this exercise, the second of (17) is used directly to evaluate $r_{ii,k} r_{ii,l}$ at the end points, while it is used at the nodal point in conjunction with a Richardson extrapolation[23] of the form

$$r_{ii,k}^{(n)} r_{ii,l}^{(n)} = \frac{1}{2}[-r_{i(i-\epsilon),k} r_{i(i-\epsilon),l} + 2 r_{i(i-2\epsilon),k} r_{i(i-2\epsilon),l} + 2 r_{i(i+2\epsilon),k} r_{i(i+2\epsilon),l} - r_{i(i+\epsilon),k} r_{i(i+\epsilon),l}] \tag{20}$$

where $r_{i(i-\epsilon),k}$, for example, denotes the value of $r_{ii,k}$ [obtained from the second of (17)] that pertains to the ith nodal point and to a fixed point located between the nodal points $i-1$ and i at a distance ϵ from nodal point i; here, ϵ has been taken as $0.05\, L_i$.

Finally, each value of F_{ij}^{kl} is scaled through division by L_j. This scales the tractions t_j^k so that they, in effect, become nodal forces, producing a stiffness matrix $\underline{K}_m$ of the standard FE form.